Advances in Computer Science Research, volume 88
International Conference on Computer, Network, Communication and Information Systems (CNCI 2019)

Global Fast Terminal Sliding Mode Control Law Design of a Quadrotor

Hwachou Chen[1, a], Haiyun Chen[1, 2, b] and Ping Xu[3, c]

[1]School of Electrical Engineering and Information, Southwest Petroleum University, Chengdu 610500, China

[2]Southwest Petroleum University (Nanchong), Nanchong 637001, China

[3]State Grid Szechuan Electric Power Company Guangyuan Power Supply Company, Guangyuan, 628000, China

[a]hwachou@163.com, [b]1921600392@qq.com, [c]602201216@qq.com

Abstract. The conventional sliding mode control cannot converge to zero in finite time, and it has a feeble robustness because of its linear sliding mode surface with uncertain variable disturbances, in order to solve these problems, this paper presents an adaptive global fast terminal sliding mode control (GFTSMC) based on a quadrotor UAV. Firstly, the mathematical model of quadrotor is given via Euler-Lagrange method. A double closed-loop structure is designed, the GFTSMC laws are formulated in the outer loop controller to track the position signal, and to track the attitude signal in the inner loop controller. To eliminate the chattering, the sign function is replaced by a saturation function. The stability of system is proved by Lyapunov method. Finally, the demonstrative simulation results are shown to embody the superiorities of GFTSMC compared with the classical sliding mode control (CSMC).

Keywords: Quadrotor UAV, Global Fast Terminal SMC, Trajectory Tracking, Lyapunov Method, Adaptive Law

1. Introduction

Quadrotor Unmanned Aerial Vehicle, which has four rotors symmetrically distribute on the body of the aircraft has been widely applied in military and civil fields, such as fire surveillance, earthquake disaster relief, agricultural plant protection, law enforcement, mapping and military reconnaissance, etc. The quadrotor is a strong coupling, under-actuated and nonlinear intricate system, and these complex characteristics have drawn many researchers' enthusiasm and interest to it. There are lots of methods for controlling the quadrotor system, the classical PID control strategy was applied to such a nonlinear system in references [1-2]. Due to the control strategy itself, the system would work normally only with the approximate linear dynamics and micro-disturbances. Jeong S. and Jung S. studied the image processing and machine vision, the position control and indoor positioning of quadrotor were realized [3]. The derivative-free nonlinear Kalman filter was used for a quadrotor UAV's robust controller in [4-5], by applying Kalman filtering on the linearized equivalent of the system, the state vector of quadrotor can be estimated without computing Jacobian matrices and partial derivatives. Nguyen D. T. presented an active fault-tolerant control system in the presence of actuator faults with both fault detection and diagnosis, a two-stage Kalman filter was used to estimate the scheduled gains which are parameterized as polynomial functions of the loss of control effectiveness of the quadrotor actuators [6]. To enhance the control performance and altitude control precision, feedforward control and transition process were set on the PID feedback controller in [7]. Better control effects are shown on these methods than traditional PID control, but there are still some unsolved problems such as strong coupling, response speed, error convergence and so on. Shakev and Topalov designed a continuous sliding mode controller based on Lyapunov method, this controller for quadrotor has an advantage that it is not being sensitive to model errors, parametric uncertainties and other disturbances [8]. But the chattering phenomenon is inevitable in conventional linear sliding mode control. The system state variables have a desired error dynamics which is guaranteed by defining that the conventional linear

sliding mode is a linear combination between the position error and velocity error of system state variables. The sliding mode surface is a linear hyperplane, although the asymptotic convergence of error dynamics can be guaranteed, the error dynamics cannot converge to zero in finite-time. To eliminate the chattering, a real-time robust altitude control scheme and a fuzzy logic control were presented in [9-11] for the efficient performance of a quadrotor aircraft system using continuous sliding mode control and quasi sliding mode control respectively. Kidouche and Riache et al. in [12-14] developed an adaptive super-twisting sliding mode control algorithm to control the quadrotor helicopter to track desired attitudes under various conditions, this method enhanced the robustness of the system. In references [15-20], the quadrotor system state equation was divided into under-actuated subsystem and fully actuated subsystem, and a fast terminal sliding mode control was proposed to converge the system statuses in finite time. However, the chattering phenomenon has not been restrained completely. In fact, it is not a direct linear relationship between the disturbances and control inputs, the stability cannot be guaranteed by switching the sliding mode robust terms, so it's necessary to design an adaptive law for the disturbances. In this work, adaptive laws are designed to estimate the mass of quadrotor UAV and disturbances. In most of the existing literatures on attitude control and trajectory tracking of quadrotor aerocraft focus on stability and robustness of the system, however there are few researches on finite time convergence control. Fast terminal sliding mode control is applied to a quadrotor UAV in this paper, and the finite time convergence control is realized.

2. Mathematic Model of Quadrotor

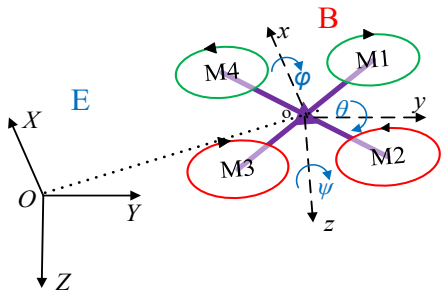

Fig. 1 Configuration and Coordinates of Quadrotor UAV

As is shown in Fig.1, four propellers at the endpoints of the quadrotor UAV's crossover structure respectively. To offset the rotational counter torque, M1 and M3 are clockwise while M2, M4 are anticlockwise. We should consider two coordinate systems before modeling the quadrotor: the body coordinate and the earth coordinate as is shown in Fig. 1.

The rotation matrix $\boldsymbol{R}_{\mathrm{B}\to\mathrm{E}}$ which transforms the body coordinate system to earth coordinate system is defined as follows:

$$\boldsymbol{R}_{\mathrm{B}\to\mathrm{E}}=\begin{bmatrix} \mathrm{C}\theta\mathrm{C}\psi & \mathrm{S}\phi\mathrm{S}\theta\mathrm{C}\psi-\mathrm{C}\phi\mathrm{S}\psi & \mathrm{C}\phi\mathrm{S}\theta\mathrm{C}\psi+\mathrm{S}\phi\mathrm{S}\psi \\ \mathrm{C}\theta\mathrm{S}\psi & \mathrm{S}\phi\mathrm{S}\theta\mathrm{S}\psi+\mathrm{C}\phi\mathrm{C}\psi & \mathrm{C}\phi\mathrm{S}\theta\mathrm{S}\psi-\mathrm{S}\phi\mathrm{C}\psi \\ -\mathrm{S}\theta & \mathrm{S}\phi\mathrm{C}\theta & \mathrm{C}\phi\mathrm{C}\theta \end{bmatrix} \tag{1}$$

Where C(□) is cosine and S(□) is sine, $[\phi \quad \theta \quad \psi]^{\mathrm{T}}$ represents Euler angles roll, pitch and yaw respectively.

According to Lagrange approach, the simplified model of quadrotor is given as follows:

$$\begin{cases} m\ddot{\boldsymbol{X}}=u_1\boldsymbol{R}_{\mathrm{B}\to\mathrm{E}}\boldsymbol{e}_3-mg\boldsymbol{e}_3+\boldsymbol{K}\dot{\boldsymbol{X}}+\boldsymbol{D}_1 \\ \boldsymbol{J}\ddot{\boldsymbol{\Theta}}=\boldsymbol{\Gamma}-\boldsymbol{C}\dot{\boldsymbol{\Theta}}+\boldsymbol{D}_2 \end{cases} \tag{2}$$

Where m is the total mass of the vehicle; $\boldsymbol{X}=[x \quad y \quad z]^{\mathrm{T}}$ is the space coordinate vector of the center point of quadrotor UAV; $\boldsymbol{\Theta}=[\phi \quad \theta \quad \psi]^{\mathrm{T}}$ is the Euler angles of quadrotor UAV's attitude; $\boldsymbol{e}_3=[0 \quad 0 \quad 1]^{\mathrm{T}}$ is a unit vector; the unknown disturbances $\boldsymbol{D}_1=[d_1 \quad d_2 \quad d_3]^{\mathrm{T}}$, $\boldsymbol{D}_2=[d_4 \quad d_5 \quad d_6]^{\mathrm{T}}$ attaching to each channel input separately. The coefficient matrices $\boldsymbol{K}$ is defined as:

$$\boldsymbol{K}=\begin{bmatrix}-k_1 & 0 & 0\\ 0 & -k_2 & 0\\ 0 & 0 & -k_3\end{bmatrix} \tag{3}$$

Where k_i ($i=1,2,3$) are drag coefficients.

u_1 and $\boldsymbol{\Gamma}$ are the lift force and torque inputs. The control inputs $\boldsymbol{U}=\begin{bmatrix}u_1 & u_2 & u_3 & u_4\end{bmatrix}^{\mathrm{T}}$ are defined as follows:

$$\begin{bmatrix}u_1\\ u_2\\ u_3\\ u_4\end{bmatrix}=\begin{bmatrix}u_1\\ \boldsymbol{\Gamma}\end{bmatrix}=\begin{bmatrix}\mu l & \mu l & \mu l & \mu l\\ -\mu l & -\mu l & \mu l & \mu l\\ \mu l & -\mu l & -\mu l & \mu l\\ -\upsilon & \upsilon & \upsilon & -\upsilon\end{bmatrix}\begin{bmatrix}\omega_1^2\\ \omega_2^2\\ \omega_3^2\\ \omega_4^2\end{bmatrix}=\begin{bmatrix}F_1+F_2+F_3+F_4\\ -F_1-F_2+F_3+F_4\\ F_1-F_2-F_3+F_4\\ b\left(-F_1+F_2+F_3-F_4\right)\end{bmatrix} \tag{4}$$

Where μ,υ are constants associated with aerodynamics. F_i ($i=1,2,3,4$) are the lift force generated by each propeller; ω_i ($i=1,2,3,4$) are the angular velocity of each propeller; and b is a force to moment scaling factor; l is the distance between the center of the propeller and the center of the body.

In Eq.(2), $\boldsymbol{J}$ is the moment inertia of rotating around the body coordinate axes $\boldsymbol{I}=\mathrm{diag}\begin{bmatrix}I_x & I_y & I_z\end{bmatrix}$ transformed in the earth coordinate system:

$$\boldsymbol{J}=\begin{vmatrix}I_x & 0 & -I_x\mathrm{S}\theta\\ 0 & I_y\mathrm{C}^2\phi+I_z\mathrm{S}^2\phi & \left(I_y-I_z\right)\mathrm{S}\phi\mathrm{C}\phi\mathrm{C}\theta\\ -I_x\mathrm{S}\theta & \left(I_y-I_z\right)\mathrm{S}\phi\mathrm{C}\phi\mathrm{C}\theta & I_x\mathrm{S}^2\theta+I_y\mathrm{S}^2\phi\mathrm{C}^2\theta+I_z\mathrm{C}^2\phi\mathrm{C}^2\theta\end{vmatrix} \tag{5}$$

$\boldsymbol{C}$ is the Coriolis force and centrifugal force matrix; it is formulated as Eq. (6):

$$\boldsymbol{C}=\dot{\boldsymbol{J}}-\frac{1}{2}\frac{\partial}{\partial\boldsymbol{\Theta}}\left(\dot{\boldsymbol{\Theta}}^{\mathrm{T}}\boldsymbol{J}\right) \tag{6}$$

The coupling relationships among the attitude angles are reflected by $\boldsymbol{J}$ and $\boldsymbol{C}$.

$$\begin{cases}m\ddot{x}=\left(\mathrm{C}\phi\mathrm{S}\theta\mathrm{C}\psi+\mathrm{S}\phi\mathrm{S}\psi\right)u_1-k_1\dot{x}+d_1\\ m\ddot{y}=\left(\mathrm{C}\phi\mathrm{S}\theta\mathrm{S}\psi-\mathrm{S}\phi\mathrm{C}\psi\right)u_1-k_2\dot{y}+d_2\\ m\ddot{z}=\left(\mathrm{C}\phi\mathrm{C}\theta\right)u_1-mg-k_3\dot{z}+d_3\\ \ddot{\phi}=\dot{\theta}\dot{\psi}\dfrac{I_y-I_z}{I_x}+\dfrac{J_r}{I_x}\dot{\theta}\Omega_r+\dfrac{l}{I_x}u_2-\dfrac{k_4 l}{I_x}\dot{\phi}+d_4\\ \ddot{\theta}=\dot{\phi}\dot{\psi}\dfrac{I_z-I_x}{I_y}-\dfrac{J_r}{I_y}\dot{\phi}\Omega_r+\dfrac{l}{I_y}u_3-\dfrac{k_5 l}{I_y}\dot{\theta}+d_5\\ \ddot{\psi}=\dot{\phi}\dot{\theta}\dfrac{I_x-I_y}{I_z}+\dfrac{1}{I_z}u_4-\dfrac{k_6}{I_z}\dot{\psi}+d_6\end{cases} \tag{7}$$

From the above, introduce the equations (1) and (3-6) to equation (2), and simplify it, the mathematic model of a quadrotor can be written as Eq. (7). Where $\Omega_r=-\omega_1+\omega_2-\omega_3+\omega_4$, and J_r denotes the inertia of the propeller.

3. Control Law Design

The desired objective of controller is $x\to x_d$, $y\to y_d$, $z\to z_d$, $\phi\to 0$, $\theta\to 0$, $\psi\to\psi_d$.

An inner-outer loop structure of controller is adopted; the inner loop is attitude controller, while the outer loop is position controller. The intermediate command signals ϕ_d,θ_d are generated by the position controller, the position and attitude controllers are respectively designed based on global fast terminal sliding mode control. The control structure of quadrotor UAV is shown in Fig. 2.

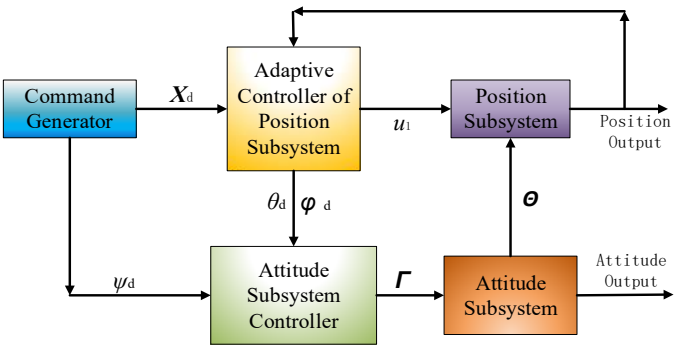

Fig. 2 Dual Closed-Loop Control Structure

3.1 Adaptive Position Controller Design.

Define a virtual control input of position subsystem:

$$\boldsymbol{U}_p = \begin{bmatrix} u_{1x} \\ u_{1y} \\ u_{1z} \end{bmatrix} = u_1 \boldsymbol{R}_{\mathrm{B}\to\mathrm{E}} \boldsymbol{e}_3 \tag{8}$$

Control law u_{1x} is designed as an illustration. The position x tracking error is

$$e_x = x_d - x \tag{9}$$

Where x_d is desired signal. The second derivative of the error is:

$$\ddot{e}_x = \ddot{x}_d - \ddot{x} = \ddot{x}_d - \frac{u_{1x} + d_1}{m} + \frac{k_1}{m}\dot{x} \tag{10}$$

Choose a sliding mode surface:

$$\sigma_1 = \dot{e}_x + \lambda_1 e_x \tag{11}$$

Where $\lambda_1 > 0$, and differentiate it:

$$\dot{\sigma}_1 = \ddot{e}_x + \lambda_1 \dot{e}_x = \ddot{x}_d - \frac{u_{1x} + d_1}{m} + \frac{k_1}{m}\dot{x} + \lambda_1 \dot{e}_x \tag{12}$$

Select the global fast sliding mode surface as:

$$s_1 = \dot{\sigma}_1 + \alpha_1 \sigma_1 + \beta_1 \sigma_1^{\frac{q_1}{p_1}} \tag{13}$$

Where $\alpha_1 > 0, \beta_1 > 0$, and p_1, q_1 are odd integers, and $p_1 > q_1$ [20]. The derivative of s_1 is calculated as:

$$\dot{s}_1 = \ddot{\sigma}_1 + \alpha_1 \dot{\sigma}_1 + \beta_1 \frac{q_1}{p_1} \sigma_1^{\frac{q_1}{p_1}-1} \dot{\sigma}_1 = \dddot{e}_x + \left(\lambda_1 + \alpha_1 + \beta_1 \frac{q_1}{p_1} \sigma_1^{\frac{q_1}{p_1}-1} \right) \ddot{e}_x + \lambda_1 \left(\alpha_1 + \beta_1 \frac{q_1}{p_1} \sigma_1^{\frac{q_1}{p_1}-1} \right) \dot{e}_x \tag{14}$$

Define that

$$M_1 = \left(\lambda_1 + \alpha_1 + \beta_1 \frac{q_1}{p_1} \sigma_1^{\frac{q_1}{p_1}-1} \right), \quad N_1 = \lambda_1 \left(\alpha_1 + \beta_1 \frac{q_1}{p_1} \sigma_1^{\frac{q_1}{p_1}-1} \right) \tag{15}$$

Whereupon

$$\dot{s}_1 = \dddot{e}_x + M_1 \ddot{e}_x + N_1 \dot{e}_x = \dddot{e}_x + M_1 \left(\ddot{x}_d - \frac{u_{1x} + d_1}{m} + \frac{k_1}{m}\dot{x} \right) + N_1 \dot{e}_x \tag{16}$$

The virtual control u_{1x} is designed:

$$u_{1x} = \hat{m}\bar{u}_{1x} - \hat{d}_1 \tag{17}$$

Where

$$\bar{u}_{1x} = \frac{1}{M_1}\left(\dddot{e}_x + N_1 \dot{e}_x \right) + \ddot{x}_d + \frac{k_1}{m}\dot{x} + \xi_1 \operatorname{sgn}(s_1) + \eta_1 s_1^{\frac{q_1}{p_1}} \tag{18}$$

$\hat{m}$, $\hat{d}_1$ represent the estimated value of mass and disturbance respectively. ξ_1 and η_1 are positive coefficients. So the $\dot{s}_1$ can be rewritten as:

$$\dot{s}_1 = \dddot{e}_x + M_1\left(\ddot{x}_d - \frac{\hat{m}\bar{u}_{1x} - \hat{d}_1 + d_1}{m} + \frac{k_1}{m}\dot{x}\right) + N_1\dot{e}_x \tag{19}$$

The adaptive law can be designed as:

$$\begin{cases} \dot{\hat{d}}_1 = -M_1\gamma_1 s_1 \\ \dot{\hat{m}} = \gamma_2 M_1 s_1 \bar{u}_{1x} \end{cases} \tag{20}$$

Where γ_1 and γ_2 are positive constants. Define an error of estimated disturbance as $\tilde{d}_1 = d_1 - \hat{d}_1$, and an error of estimated mass is $\tilde{m} = m - \hat{m}$. Choose the Lyapunov function as:

$$V_1 = \frac{1}{2}s_1^2 + \frac{1}{2m\gamma_1}\tilde{d}_1^2 + \frac{1}{2m\gamma_2}\tilde{m}^2 \tag{21}$$

According to Eq.(18),

$$\dddot{e}_x + N_1\dot{e}_x + M_1\ddot{x}_d + \frac{M_1 k_1}{m}\dot{x} = M_1\left(\bar{u}_{1x} - \xi_1\,\mathrm{sgn}(s_1) - \eta_1 s_1^{\frac{q_1}{p_1}}\right) \tag{22}$$

Then

$$\dot{s}_1 = -\frac{M_1}{m}\left(\hat{m}\bar{u}_{1x} - \hat{d}_1 + d_1\right) + M_1\left(\bar{u}_{1x} - \xi_1\,\mathrm{sgn}(s_1) - \eta_1 s_1^{\frac{q_1}{p_1}}\right) \tag{23}$$

Thereupon

$$\dot{V}_1 = s_1\dot{s}_1 + \frac{1}{m\gamma_1}\tilde{d}_1\dot{\tilde{d}}_1 + \frac{1}{m\gamma_2}\tilde{m}\dot{\tilde{m}} = s_1\left[-\frac{M_1}{m}\left(\hat{m}\bar{u}_{1x} - \hat{d}_1 + d_1\right) + M_1\left(\bar{u}_{1x} - \xi_1\,\mathrm{sgn}(s_1) - \eta_1 s_1^{\frac{q_1}{p_1}}\right)\right] + \frac{1}{m\gamma_1}\tilde{d}_1\dot{\tilde{d}}_1 + \frac{1}{m\gamma_2}\tilde{m}\dot{\tilde{m}} \tag{24}$$

Assume that the disturbance and mass are slow time-varying signals, and $\dot{\tilde{d}}_1 = -\dot{\hat{d}}_1$, $\dot{\tilde{m}} = -\dot{\hat{m}}$.The derivative of Lyapunov function is:

$$\dot{V}_1 = -\frac{M_1\hat{m}}{m}s_1\bar{u}_{1x} - \frac{M_1\tilde{d}_1}{m}s_1 + M_1 s_1\bar{u}_{1x} - M_1\xi_1|s_1| - M_1\eta_1 s_1^{\frac{q_1}{p_1}+1} - \frac{1}{m\gamma_1}\tilde{d}\dot{\tilde{d}} - \frac{1}{m\gamma_2}\tilde{m}\dot{\hat{m}} \tag{25}$$

Introduce the adaptive law (20) into Eq.(25):

$$\dot{V}_1 = M_1 s_1\bar{u}_{1x}\left(1 - \frac{\hat{m}}{m}\right) + \frac{M_1}{m}s_1\tilde{d} - \frac{M_1}{m}s_1\tilde{d} - \frac{M_1\tilde{m}}{m}s_1\bar{u}_{1x} - M_1\xi_1|s_1| - M_1\eta_1 s_1^{\frac{q_1}{p_1}+1} = -M_1\xi_1|s_1| - M_1\eta_1 s_1^{\frac{q_1}{p_1}+1} \le 0 \tag{26}$$

It is an obvious fact that $\dot{V}_1 < 0$ when $s_1 \ne 0$, so V_1 reduces gradually, that is, s_1, $\tilde{d}_1$ and $\tilde{m}$ reduce gradually, and only if $s_1 = 0$, then $\dot{V}_1 = 0$.

V_1 is a constant when $s_1 = 0$ and $\dot{V}_1 = 0$, $\tilde{d}_1$, $\tilde{m}$ will not change and be bounded. Because the sliding mode function passes through $s_1 = 0$ continually, $\tilde{d}_1$ and $\tilde{m}$ will change their values in a boundedness. Hence, the convergence of $\tilde{d}_1$ and $\tilde{m}$ cannot be guaranteed.

In order to avoid an overlarge value of $\hat{m}$, the adaptive law (20) is modified in the case of the mass upper bound $m_{\max}$ is known. The discontinuous projection mapping method is applied:

$$\dot{\hat{m}} = \mathrm{proj}_{\hat{m}}\left(\gamma_2 M_1 s_1\bar{u}_{1x}\right) \tag{27}$$

Where

$$\mathrm{proj}_{\hat{m}}(\bullet)=\begin{cases}0, \text{ if } \hat{m}\geq m_{\max} \text{ and } \bullet>0\\ 0, \text{ if } \hat{m}\leq -m_{\max} \text{ and } \bullet<0\\ \text{others,}\end{cases} \tag{28}$$

The virtual control inputs u_{1y} and u_{1z} can be designed in a same way, and the adaptive laws of estimating d_2 and d_3 are designed in the same way as Eq.(20).

$$u_{1y}=\hat{m}\bar{u}_{1y}-\hat{d}_2 \tag{29}$$

Where

$$\bar{u}_{1y}=\frac{1}{M_2}\left(\ddot{e}_y+N_2\dot{e}_y\right)+\ddot{y}_d+\frac{k_2}{m}\dot{y}+\xi_2\,\mathrm{sgn}\left(s_2\right)+\eta_2 s_2^{\frac{q_2}{p_2}} \tag{30}$$

And

$$u_{1z}=\hat{m}\bar{u}_{1z}-\hat{d}_3 \tag{31}$$

Where

$$\bar{u}_{1z}=\frac{1}{M_3}\left(\ddot{e}_z+N_2\dot{e}_z\right)+\ddot{z}_d+\frac{k_3}{m}\dot{z}+\xi_3\,\mathrm{sgn}\left(s_3\right)+\eta_3 s_3^{\frac{q_3}{p_3}}+g \tag{32}$$

The real lift force u_1 and the intermediary command signal $\boldsymbol{\Theta}_d$ need to be calculated after the virtual control $\boldsymbol{U}_p$ is gain.

According to Eq.(7) and Eq.(8),

$$\begin{aligned}u_{1x}&=\left(\mathrm{C}\phi\mathrm{S}\theta\mathrm{C}\psi+\mathrm{S}\phi\mathrm{S}\psi\right)u_1\\ u_{1y}&=\left(\mathrm{C}\phi\mathrm{S}\theta\mathrm{S}\psi-\mathrm{S}\phi\mathrm{C}\psi\right)u_1\\ u_{1z}&=\left(\mathrm{C}\phi\mathrm{C}\theta\right)u_1\end{aligned} \tag{33}$$

Take $u_1=\frac{u_{1z}}{\mathrm{C}\phi\mathrm{C}\theta}$ into Eq. (33):

$$\begin{aligned}u_{1x}&=\frac{u_{1z}}{\mathrm{C}\phi\mathrm{C}\theta}\left(\mathrm{C}\phi\mathrm{S}\theta\mathrm{C}\psi+\mathrm{S}\phi\mathrm{S}\psi\right)=u_{1z}\left(\tan\theta\mathrm{C}\psi+\mathrm{S}\psi\tan\phi\sec\theta\right)=u_{1z}\begin{bmatrix}\mathrm{C}\psi & \mathrm{S}\psi\end{bmatrix}\begin{bmatrix}\tan\theta\\ \tan\phi\sec\theta\end{bmatrix}\\ u_{1y}&=\frac{u_{1z}}{\mathrm{C}\phi\mathrm{C}\theta}\left(\mathrm{C}\phi\mathrm{S}\theta\mathrm{S}\psi-\mathrm{S}\phi\mathrm{C}\psi\right)=u_{1z}\left(\tan\theta\mathrm{S}\psi-\mathrm{C}\psi\tan\phi\sec\theta\right)=u_{1z}\begin{bmatrix}\mathrm{S}\psi & -\mathrm{C}\psi\end{bmatrix}\begin{bmatrix}\tan\theta\\ \tan\phi\sec\theta\end{bmatrix}\end{aligned} \tag{34}$$

That is

$$\begin{bmatrix}u_{1x}\\ u_{1y}\end{bmatrix}=u_{1z}\begin{bmatrix}\mathrm{C}\psi & \mathrm{S}\psi\\ \mathrm{S}\psi & -\mathrm{C}\psi\end{bmatrix}\begin{bmatrix}\tan\theta\\ \tan\phi\sec\theta\end{bmatrix} \tag{35}$$

Substitute the intermediary command signal $\boldsymbol{\Theta}_d$ for $\boldsymbol{\Theta}$, the virtual control inputs are given:

$$\begin{bmatrix}u_{1x}\\ u_{1y}\end{bmatrix}=u_{1z}\begin{bmatrix}\mathrm{C}\psi_d & \mathrm{S}\psi_d\\ \mathrm{S}\psi_d & -\mathrm{C}\psi_d\end{bmatrix}\begin{bmatrix}\tan\theta_d\\ \tan\phi_d\sec\theta_d\end{bmatrix} \tag{36}$$

Both sides of the equation (36) are pre-multiplied by $\begin{bmatrix}\mathrm{C}\psi_d & \mathrm{S}\psi_d\end{bmatrix}$ respectively, we can obtain $u_{1x}\mathrm{C}\psi_d+u_{1y}\mathrm{S}\psi_d=u_{1z}\tan\theta_d$. Make a hypotheses that the range of θ_d and ϕ_d is $\left(-\pi/2,\ \pi/2\right)$.

Accordingly, the command signal of pitch angle is

$$\theta_d=\arctan\left(\frac{u_{1x}\mathrm{C}\psi_d+u_{1y}\mathrm{S}\psi_d}{u_{1z}}\right) \tag{37}$$

Both sides of the equation (36) are pre-multiplied by $\begin{bmatrix}\mathrm{S}\psi_d & -\mathrm{C}\psi_d\end{bmatrix}$ respectively, we can obtain $u_{1x}\mathrm{S}\psi_d-u_{1y}\mathrm{C}\psi_d=u_{1z}\frac{\tan\phi_d}{\mathrm{C}\theta_d}$.

The command signal of roll angle is

$$\phi_d = \arctan\left(\mathrm{C}\theta_d \frac{u_{1x}\mathrm{S}\psi_d - u_{1y}\mathrm{C}\psi_d}{u_{1z}} \right) \tag{38}$$

The command signal of yaw angle ψ_d is given by the remote control to track any yaw angles. The real position controller is designed as

$$u_1 = \frac{u_{1z}}{\mathrm{C}\phi_d \mathrm{C}\theta_d} \tag{39}$$

The adaptive position controller has been designed up to now. It needs to be cleared that, all 6 degrees of freedom cannot be tracked because of the underactuation. A reasonable control scheme tracks the position $\boldsymbol{P}$ and yaw angle ψ_d, and the other two Euler angles need to be bounded. Therefore the intermediary command signals ϕ_d and θ_d are not desired signals, but command signals, which are generated by the virtual control, for the attitude subsystem.

3.2 Attitude Controller Design.

The attitude control system is inner-loop subsystem, the command signals ϕ_d and θ_d generated by outer-loop are tracked by the inner-loop controller.

A global fast terminal sliding mode controller of attitude is deduced based on model (7). The control law of roll channel is computed out as an example.

Define the attitude error is

$$\boldsymbol{e_\Theta} = \begin{bmatrix} e_\phi \\ e_\theta \\ e_\psi \end{bmatrix} = \begin{bmatrix} \phi_d - \phi \\ \theta_d - \theta \\ \psi_d - \psi \end{bmatrix} \tag{40}$$

The second order derivative of roll error is

$$\ddot{e}_\phi = \ddot{\phi}_d - \ddot{\phi} = \ddot{\phi}_d - \dot{\theta}\dot{\psi}\frac{I_y - I_z}{I_x} - \frac{J_r}{I_x}\dot{\theta}\Omega_r - \frac{l}{I_x}u_2 + \frac{k_4 l}{I_x}\dot{\phi} - d_4 \tag{41}$$

Choose a sliding mode as

$$\sigma_4 = \dot{e}_\phi + \lambda_4 e_\phi \tag{42}$$

Where $\lambda_4 > 0$, and the derivative of σ_4 is given:

$$\dot{\sigma}_4 = \ddot{e}_\phi + \lambda_4 \dot{e}_\phi = \ddot{\phi}_d - \ddot{\phi} + \lambda_4 \dot{e}_\phi = \ddot{\phi}_d - \dot{\theta}\dot{\psi}\frac{I_y - I_z}{I_x} - \frac{J_r}{I_x}\dot{\theta}\Omega_r - \frac{l}{I_x}u_2 + \frac{k_4 l}{I_x}\dot{\phi} - d_4 + \lambda_4 \dot{e}_\phi \tag{43}$$

The fast terminal sliding mode surface is formulated as:

$$s_4 = \dot{\sigma}_4 + \alpha_4 \sigma_4 + \beta_4 \sigma_4^{\frac{q_4}{p_4}} \tag{44}$$

Where $\alpha_4 > 0, \beta_4 > 0$, and p, q are odd integers, and $p > q$. The derivative of s_4 is calculated as:

$$\begin{aligned} \dot{s}_4 &= \ddot{\sigma}_4 + \alpha_4 \dot{\sigma}_4 + \beta_4 \frac{q_4}{p_4}\sigma_4^{\frac{q_4}{p_4}-1}\dot{\sigma}_4 = \ddot{e}_\phi + \lambda_4 \ddot{e}_\phi + \left(\alpha_4 + \beta_4 \frac{q_4}{p_4}\sigma_4^{\frac{q_4}{p_4}-1} \right)\dot{\sigma}_4 \\ &= \ddot{e}_\phi + \begin{bmatrix} \ddot{\phi}_d - \dot{\theta}\dot{\psi}\frac{I_y - I_z}{I_x} - \frac{J_r}{I_x}\dot{\theta}\Omega_r \\ -\frac{l}{I_x}u_2 + \frac{k_4 l}{I_x}\dot{\phi} - d_4 \end{bmatrix} \left(\lambda_4 + \alpha_4 + \beta_4 \frac{q_4}{p_4}\sigma_4^{\frac{q_4}{p_4}-1} \right) + \lambda_4 \dot{e}_\phi \left(\alpha_4 + \beta_4 \frac{q_4}{p_4}\sigma_4^{\frac{q_4}{p_4}-1} \right) \end{aligned} \tag{45}$$

Define that

$$M_4 = \left(\lambda_4 + \alpha_4 + \beta_4 \frac{q_4}{p_4}\sigma_4^{\frac{q_4}{p_4}-1} \right), \quad N_4 = \lambda_4 \left(\alpha_4 + \beta_4 \frac{q_4}{p_4}\sigma_4^{\frac{q_4}{p_4}-1} \right) \tag{46}$$

Whereupon

$$\dot{s}_4 = \ddot{\sigma}_4 + \alpha_4 \dot{\sigma}_4 + \beta_4 \frac{q_4}{p_4}\sigma_4^{\frac{q_4}{p_4}-1}\dot{\sigma}_4 = \ddot{e}_\phi + M_4 \left[\ddot{\phi}_d - \dot{\theta}\dot{\psi}\frac{I_y - I_z}{I_x} - \frac{J_r}{I_x}\dot{\theta}\Omega_r - \frac{l}{I_x}u_2 + \frac{k_4 l}{I_x}\dot{\phi} - d_4 \right] + N_4 \dot{e}_\phi \tag{47}$$

The control law of roll channel u_2 is formulated as:

$$u_2 = \frac{I_x}{M_4 l}\left(\ddot{e}_\phi + N_4\dot{e}_\phi\right) + \frac{1}{l}\left[I_x\ddot{\phi}_d - \left(I_y - I_z\right)\dot{\theta}\dot{\psi} - J_r\dot{\theta}\Omega_r\right] + k_4\dot{\phi} - \xi_4\,\mathrm{sgn}\left(s_4\right) - \eta_4 s_4^{\frac{q_4}{p_4}} \tag{48}$$

Where ξ_1 and η_1 are positive coefficients. Take Eq.(48) into Eq.(47), $\dot{s}_4$ is calculated as:

$$\dot{s}_4 = -\xi_4\,\mathrm{sgn}\left(s_4\right) - \eta_4 s_4^{\frac{q_4}{p_4}} - M_4 d_4 = -\xi_4\,\mathrm{sgn}\left(s_4\right) - \gamma_4 s_4^{\frac{q_4}{p_4}} \tag{49}$$

Where $\gamma_4 = \eta_4 - \frac{d_4}{s_4^{q/p}}$, choose a Lyapunov function V_4 as:

$$V_4 = \frac{1}{2}s_4^2 \tag{50}$$

η_4 can be chosen as

$$\eta_4 = \frac{D_{\max}}{\left\|s_4^{q_4/p_4}\right\|} + \delta_4 \tag{51}$$

Where $D_{\max}$ is the bound of disturbance, $\left|d_i\right| < D_{\max}$, $(i = 1,2,...,6)$; δ is a positive constant. Thus we can obtain $\gamma_4 > 0$.

Differentiating V_4 with respect to time:

$$\dot{V}_4 = s\dot{s} = -\xi_4\left|s_4\right| - \gamma_4 s_4^{\frac{q_4}{p_4}+1} \tag{52}$$

It is obvious that $\dot{V}_4 \le 0$, so the system is stable.
According to Eq.(51), we can obtain:

$$\left\|s_4\right\| < \left(\frac{D_{\max}}{\eta_4}\right)^{\frac{p_4}{q_4}} \tag{53}$$

The errors of attitude subsystem states are guaranteed to converge to zero in a short time. According to reference [19], the time to reach the equilibrium $s_4 = 0$ is

$$t_{s_4} = \frac{p_4}{\xi_4\left(p_4 - q_4\right)}\ln\frac{\xi_4\left(s_4^{\frac{p_4-q_4}{p_4}}(0) + \gamma_4\right)}{\gamma_4} \tag{54}$$

Because $\gamma_4 > \delta_4$,

$$\ln\frac{\xi_4\left(s_4^{\frac{p_4-q_4}{p_4}}(0) + \gamma_4\right)}{\gamma_4} < \ln\frac{\xi_4\left(s_4^{\frac{p_4-q_4}{p_4}}(0) + \delta_4\right)}{\delta_4} \tag{55}$$

Therefore, the reaching time

$$t_{s_4} < \ln\frac{\xi_4\left(s_4^{\frac{p_4-q_4}{p_4}}(0) + \delta_4\right)}{\delta_4} \tag{56}$$

The control laws of pitch and yaw are given in a similar way.

$$u_3 = \frac{I_y}{M_5 l}\left(\ddot{e}_\theta + N_5\dot{e}_\theta\right) + \frac{1}{l}\left[I_y\ddot{\theta}_d - \left(I_z - I_x\right)\dot{\phi}\dot{\psi} - J_r\dot{\phi}\Omega_r\right] + k_5\dot{\theta} - \xi_5\,\mathrm{sgn}\left(s_5\right) - \eta_5 s_5^{\frac{q_5}{p_5}} \tag{57}$$

$$u_4 = \frac{I_z}{M_6}\left(\ddot{e}_\psi + N_6\dot{e}_\psi\right) + I_z\ddot{\psi}_d - \left(I_x - I_y\right)\dot{\phi}\dot{\theta} + k_6\dot{\psi} - \xi_6\,\mathrm{sgn}\left(s_6\right) - \eta_6 s_6^{\frac{q_6}{p_6}} \tag{58}$$

In the inner loop controller, errors of attitude angles, especially the initial errors, will affect the

stability of outer loop, and affect the whole system consequently. To carry out a sliding mode control of inner loop with fast convergence, a strategy of inner loop's convergence velocity greater than the convergence velocity of outer loop is applied, and the stability of the closed-loop system is guaranteed. The convergence speed of inner loop greater than the convergence speed of outer loop is guaranteed by adjusting the gain coefficient of inner loop.

4. Simulation Analysis

Make an assumption that the desired position is

$$\boldsymbol{X}_d = \left[3\cos\left(\frac{t}{2}\right), 2\sin\left(\frac{1}{2}\right), 2+\frac{t}{2}\right]^{\mathrm{T}}$$

The desired attitude is

$$\boldsymbol{\Theta}_d = \left[0, 0, \frac{\pi}{3}\right]^{\mathrm{T}}$$

The inertial matrix is

$$\boldsymbol{I} = \mathrm{diag}(1.5, 1.5, 3.2)$$

The radius of quadrotor UAV is $l = 0.5\mathrm{m}$.The simulation time is 30s, the mass m of quadrotor UAV changes every 10s.

$$m = \begin{cases} 8\mathrm{kg}, & 0 \le t < 10\mathrm{s} \\ 7\mathrm{kg}, & 10\mathrm{s} \le t < 20\mathrm{s} \\ 6\mathrm{kg}, & 20\mathrm{s} \le t \le 30\mathrm{s} \end{cases}$$

The external slow time-varying aerodynamic disturbances torque is

$$\boldsymbol{D}_1 = \begin{bmatrix} 0.2\sin(0.1\pi t) \\ 0.1\sin(0.2\pi t) \\ 0.3\cos(0.1\pi t) \end{bmatrix}, \boldsymbol{D}_2 = \begin{bmatrix} 0.3\sin(0.3\pi t)+0.5 \\ 0.4\cos(0.2\pi t)+0.2 \\ 0.5\cos(0.1\pi t)+0.2 \end{bmatrix}$$

What needs illustration is that these coefficients would be changed for implementing different control performances.

Replace the switching function $\mathrm{sgn}(s)$ with saturation function $\mathrm{sat}(s)$, and the boundary thickness $\Delta = 0.2$.

The simulation block diagram of control system which is built in MATLAB/Simulink is shown as Fig. 3. This is a dual closed-loop system; the inner loop is attitude subsystem, while the outer loop is position subsystem.

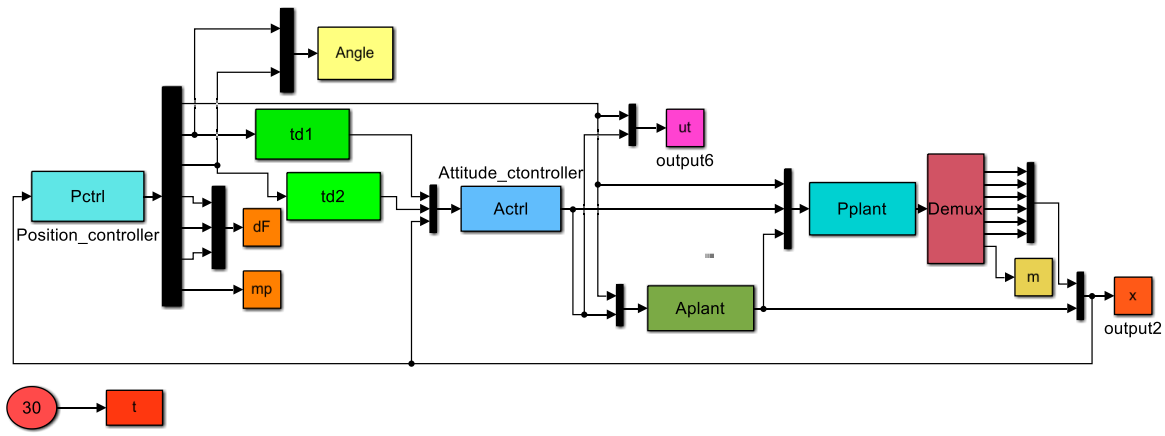

Fig. 3 Simulation Block Diagram of Control System

Make comparisons between CSMC and adaptive GFTSMC with dual closed loops to illustrate the high performance of adaptive GFTSMC with dual closed loops. When system parameters change may occur the instability, so we set an invariable mass in CSMC system. The trajectory of position tracking using CSMC is shown in Fig. 4(a) and Fig. 5(a), while Fig. 4(b) and Fig. 5(b)

show the trajectory of position tracking by using GFTSMC. As is shown in Fig. 4(b), when the mass of quadrotor UAV changes, the trajectory of position tracking has a subtle deviation. Even so, the position tracking by using GFTSMC is distinctly better than it by using CSMC. This conclusion can be further confirmed in Fig. 5(a) and Fig5(b). The red dotted line is desired position, and the blue solid line is true tracking trajectory. In Fig. 5(a), the desired trajectories of x, y and z are tracked after about 1.5s. Visibly, there is a gap between the red dotted line and the blue solid line, and they don't coincide. But in Fig. 5(b), the result is much better. The desired trajectory of x is tracked by x after about 1.5s, and the desired trajectories of y and z are tracked after about 0.5s, the tracking time is shortened availably. And the blue solid line and the red dotted line almost coincide.

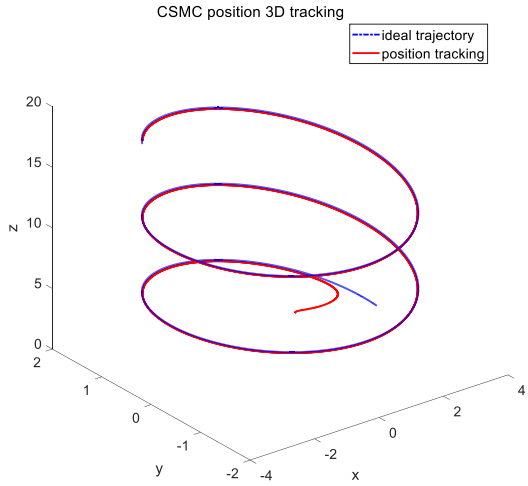

Fig. 4 (a) Position Tracking by CSMC

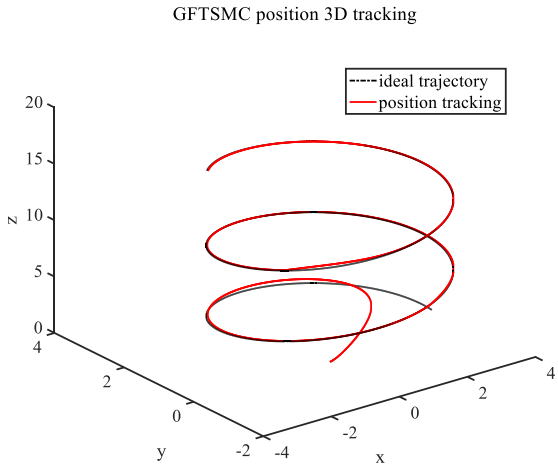

Fig. 4 (b) Position Tracking by GFTSMC

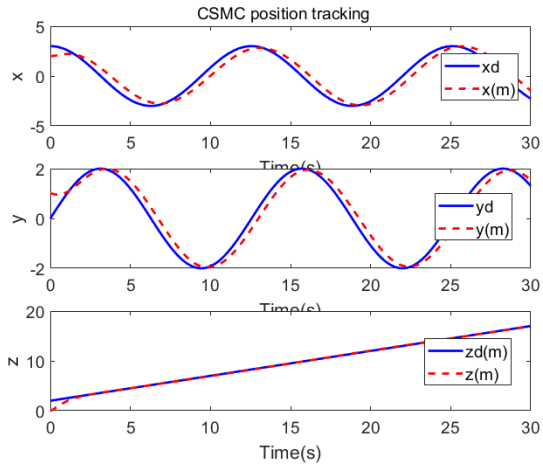

Fig. 5 (a) Position Tracking by CSMC

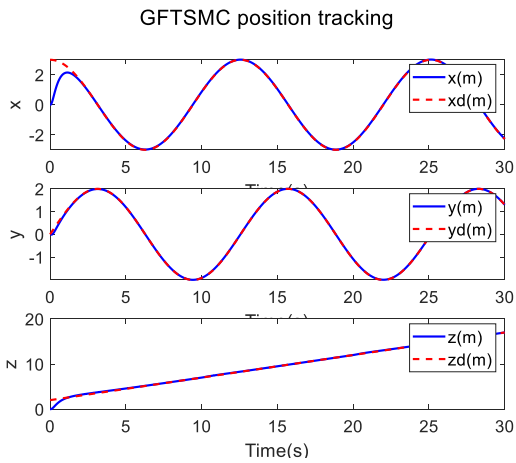

Fig. 5 (b) Position Tracking by GFTSMC

There is a problem with classical sliding mode control that the errors would not converge to zero in a finite time. As is shown in Fig. 6(a), the error e_x and e_y are vibrating in a boundary of (-0.5, 0.5), while the error e_z is about -0.2. Errors converge to zero in a finite time by using adaptive global fast terminal sliding mode control, as is shown in Fig. 6(b). When $t = 10\text{s}$ and $t = 20\text{s}$, the errors have a little variation because of the change of mass, but they converge to zero quickly.

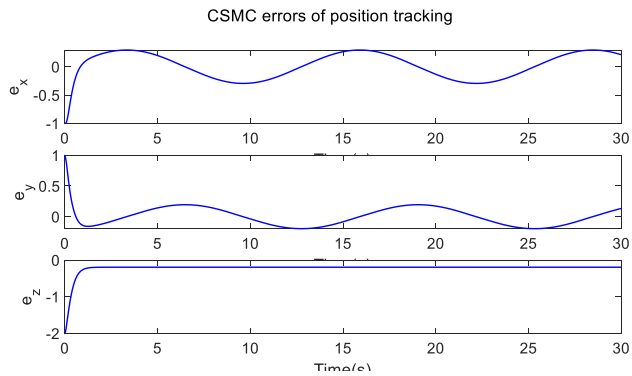

Fig. 6 (a) Errors of Position Tracking by CSMC

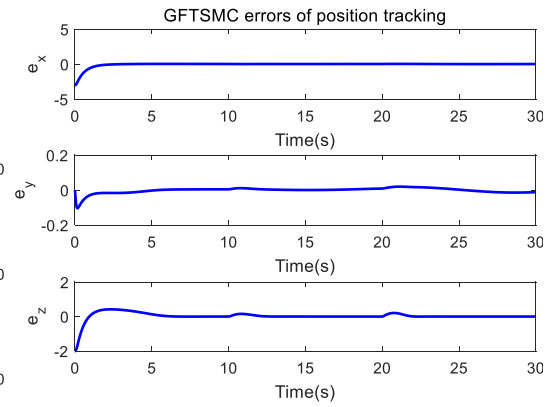

Fig.6 (b) Errors of Position Tracking by GFTSMC

Fig. 7 (a) shows the tracking trajectories of attitude angles ϕ, θ and ψ controlled by CSMC, and Fig. 7(b) shows those controlled by GFTSMC. In Fig. 7(a), the roll angle ϕ tracks its desired signal ϕ_d at $t=2.1\text{s}$, pitch angle θ tracks its desired signal θ_d at $t=1.2\text{s}$, yaw angle ψ tracks its desired signal ψ_d at $t=0.3\text{s}$. In Fig.7(b), the roll angle ϕ tracks its desired signal ϕ_d at $t=1.5\text{s}$, pitch angle θ tracks its desired signal θ_d at $t=1.3\text{s}$, yaw angle ψ tracks its desired signal ψ_d at $t=0.15\text{s}$. As we can see, there is a large high frequency oscillations in CSMC before it is stable and the attitude errors cannot converge to zero in the whole process of tracking.

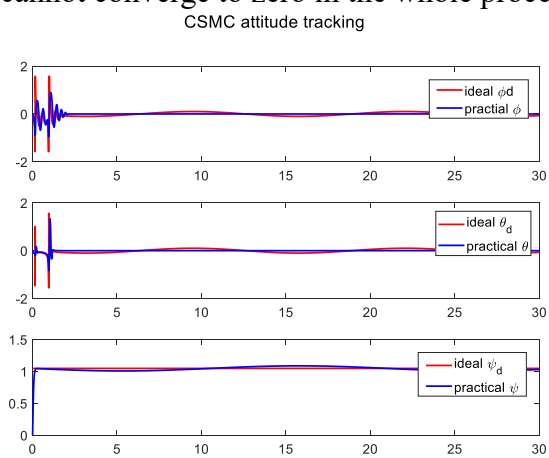

Fig. 7 (a) Attitude Tracking by CSMC

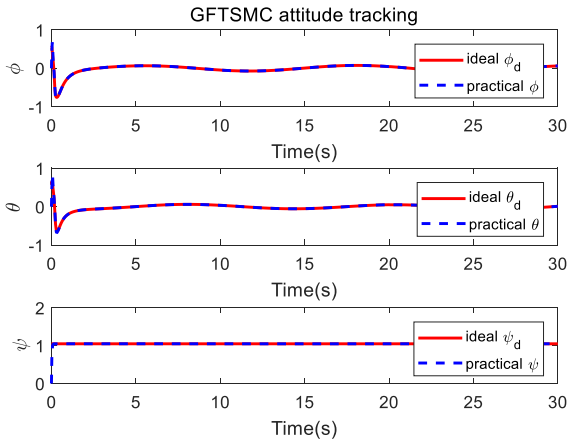

Fig. 7 (b) Attitude Tracking by GFTSMC

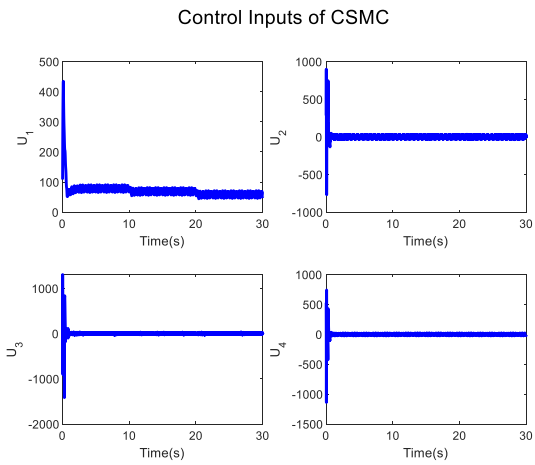

Fig. 8 (a) CSMC Inputs

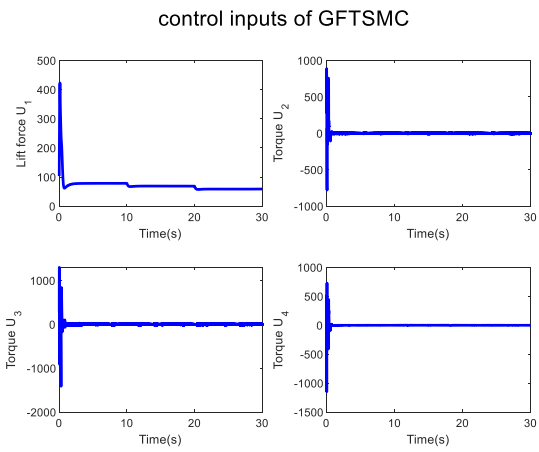

Fig. 8 (b) GFTSMC Inputs

Fig. 8 (a) shows four control inputs of CSMC based on a duel closed-loop structure. And Fig. 8 (b) shows four control inputs $\boldsymbol{U}=[u_1 \quad u_2 \quad u_3 \quad u_4]^{\mathrm{T}}$ of GFTSMC. As is shown, when the mass changes at time t=10s and t=20s, the inputs have a slight change.

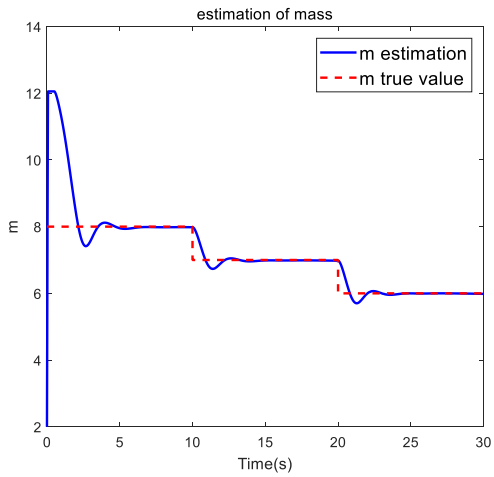

Fig. 9 (a) Adaptive Estimation of Mass

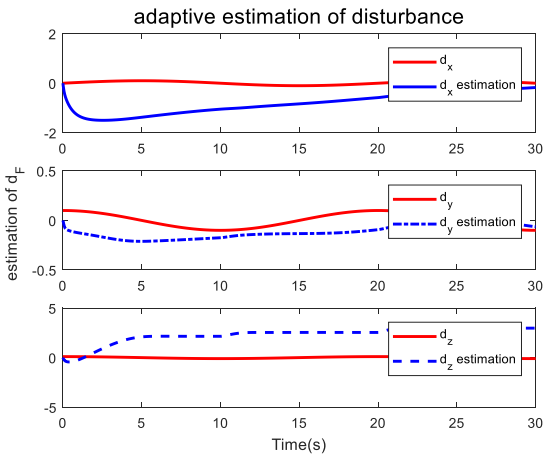

Fig. 9 (b) Adaptive Estimation of Disturbances

The adaptive parameter estimation of mass m and disturbances $\boldsymbol{D_1}$ are shown in Fig. 9 (a) and Fig. 9 (b). The error of mass estimation is very small, and the errors of $[d_1 \quad d_2 \quad d_3]^{\mathrm{T}}$ are within an acceptable limits, which will not affect the performance of control system.

5. Conclusion

The global fast terminal sliding mode control laws based on a quadrotor UAV are designed in this paper, and adaptive laws are designed to estimate the mass and disturbances. The system of quadrotor UAV is divided into position subsystem and attitude subsystem, and an adaptive law is designed to estimate the parameters of mass and uncertain disturbances. The desired angle signals ϕ_d and θ_d which generated by position controller input into attitude controller. A saturation function $\mathrm{sat}(s)$ is applied to substitute for the switching function $\mathrm{sgn}(s)$, consequently, the chattering phenomenon is effectively restrained. The superiorities of GFTSMC are demonstrated contrastively in MATALB simulation results. But the tracking time of x is still a little bit long in Fig. 7, further optimization will be carried out in the following studies.

According to the results in Fig. 9(b), the adaptive estimation algorithm for disturbances needs to be improved, although the errors are very small.

The dynamic model of quadrotor UAV in this paper is an idealized model, some system variables such as gyroscopic effects of motors and propellers are ignored, but this does not affect the stability and control performance of the system. The adaptive global fast terminal sliding mode control is not sensitive to the uncertainty of system parameters, and it has a strong robustness, in practice, the control strategy proposed in this paper can be applied to the real quadrotor UAV.

The mass of plant protection UAV is real-time varying, so the adaptive parameter estimation provided in this paper is of great practical significance to such UAVs.

Although the control effects of other versions of SMC are not better than this work, even the chattering phenomenon is not effectively restrained, the control effects satisfy the requirements to a certain extent and easy to implement.

This research is supported by the foundation of Nanchong City-School Strategic Cooperation Project of Science and Technology (NC17SY4011), which we heartily acknowledge. And I express my sincere thanks to my parents for their support. And thank for professor CHEN Hai-yun, for teaching.

References

[1]. Yang S, Wang Z. Quad-Rotor UAV Control Method Based on PID Control Law[C]// International Conference on Computer Network, Electronic and Automation. IEEE Computer Society, 2017:418-421.

[2]. Du W Y, Jian Z Z, Chen T X. The design of flight control law based on integral separation PID algorithm[C]// International Conference on Electronics and Optoelectronics. IEEE, 2011:V2-442-V2-444.

[3]. Jeong S, Jung S. Vision-based localization of a quad-rotor system[C]// 9th International Conference on Ubiquitous Robots and Ambient Intelligence (URAI), IEEE, Daejeon, Korea, 2012, 636-638,

[4]. Rigatos G, Siano P. Control of Quadrotors with the Use of the Derivative-Free Nonlinear Kalman Filter[J]. Intelligent Industrial Systems, 2015, 1(4):275-287.

[5]. Tarhan M, Altuğ E. EKF Based Attitude Estimation and Stabilization of a Quadrotor UAV Using Vanishing Points in Catadioptric Images[J]. Journal of Intelligent & Robotic Systems, 2011, 62(3-4):587-607.

[6]. Nguyen D T, Saussie D, Saydy L. Quaternion-based robust fault-tolerant control of a quadrotor UAV[C]// International Conference on Unmanned Aircraft Systems, Miami, FL, USA. IEEE, 2017:1333-1342

[7]. Dong H R, Li B. Altitude control algorithm design of the quadrotor aircraft[C]// Chinese Automation Congress. 2017:6022-6026.

[8]. Shakev N G, Topalov A V. Continuous Sliding Mode Control of a Quadrotor[M]// Recent Advances in Sliding Modes: From Control to Intelligent Mechatronics. Springer International Publishing, 2015:441-458.

[9]. González I, Salazar S, Lozano R. Chattering-Free Sliding Mode Altitude Control for a Quad-Rotor Aircraft: Real-Time Application[J]. Journal of Intelligent & Robotic Systems, 2014, 73(1-4):137-155.

[10]. Ammar N B, Bouallègue S, Haggège J, et al. Chattering Free Sliding Mode Controller Design for a Quadrotor Unmanned Aerial Vehicle[J]. 2017.

[11]. Zeghlache S, Saigaa D, Kara K, et al. Fuzzy Sliding Mode Control with Chattering Elimination for a Quadrotor Helicopter in Vertical Flight[J]. Springer, Verlag Berlin Heidelberg, 2012, 7208:125-136.

[12]. Kidouche M, Riache S, Rezoug A. Adaptive Sliding Mode Control for Quadrotor Helicopter[C]// International Conference on Technological Advances in Electrical Engineering. 2016.

[13]. Islam S, Faraz M, Ashour R K, et al. Adaptive sliding mode control design for quadrotor unmanned aerial vehicle[C]// International Conference on Unmanned Aircraft Systems. IEEE, 2015:34-39.

[14]. Hoang V T. Adaptive Twisting Sliding Mode Control for Quadrotor Unmanned Aerial Vehicles[C]// Asian Control Conference. 2017. 611-676

[15]. Wang G X, Sui H H. TSMC Based Wind Resistance Research for Quad-Rotor UAVs[J]. Electronics Optics & Control, 2018. 25(3):87-91

[16]. Jiang H, Guan P, Xinsheng G E, et al. Attitude control of aircraft based on fast terminal sliding mode[J]. Journal of Beijing Information Science & Technology University, 2017, 32(4):29-34.

[17]. Ye D, Wang Q, Li J. Fast sliding mode tracking control of micro quadrotor UAV[C]// Control and Decision Conference. IEEE, 2016:632-636.

[18]. Xiong J J, Zhang G B. Global fast dynamic terminal sliding mode control for a quadrotor UAV[J]. Isa Transactions, 2016, 66:233-240.